AMERICAN SOCIETY FOR MICROBIOLOGY | Journal of Bacteriology

L-Arginine Modifies the Exopolysaccharide Matrix and Thwarts *Streptococcus mutans* Outgrowth within Mixed-Species Oral Biofilms

Jinzhi He,[a,b] Geelsu Hwang,[b] Yuan Liu,[b] Lizeng Gao,[b] LaTonya Kilpatrick-Liverman,[c] Peter Santarpia,[c] Xuedong Zhou,[a] Hyun Koo[b]

State Key Laboratory of Oral Diseases, Department of Endodontics, West China Hospital of Stomatology, Sichuan University, Chengdu, China[a]; Biofilm Research Labs, Levy Center for Oral Health, Department of Orthodontics and Divisions of Pediatric Dentistry and Community Oral Health, University of Pennsylvania School of Dental Medicine, Philadelphia, Pennsylvania, USA[b]; Colgate-Palmolive Technology Center, Piscataway, New Jersey, USA[c]

ABSTRACT

L-Arginine, a ubiquitous amino acid in human saliva, serves as a substrate for alkali production by arginolytic bacteria. Recently, exogenous L-arginine has been shown to enhance the alkalinogenic potential of oral biofilm and destabilize its microbial community, which might help control dental caries. However, L-arginine exposure may inflict additional changes in the biofilm milieu when bacteria are growing under cariogenic conditions. Here, we investigated how exogenous L-arginine modulates biofilm development using a mixed-species model containing both cariogenic (*Streptococcus mutans*) and arginolytic (*Streptococcus gordonii*) bacteria in the presence of sucrose. We observed that 1.5% (wt/vol) L-arginine (also a clinically effective concentration) exposure suppressed the outgrowth of *S. mutans*, favored *S. gordonii* dominance, and maintained *Actinomyces naeslundii* growth within biofilms (versus vehicle control). In parallel, topical L-arginine treatments substantially reduced the amounts of insoluble exopolysaccharides (EPS) by >3-fold, which significantly altered the three-dimensional (3D) architecture of the biofilm. Intriguingly, L-arginine repressed *S. mutans* genes associated with insoluble EPS (*gtfB*) and bacteriocin (*SMU.150*) production, while *spxB* expression (H_2O_2 production) by *S. gordonii* increased sharply during biofilm development, which resulted in higher H_2O_2 levels in arginine-treated biofilms. These modifications resulted in a markedly defective EPS matrix and areas devoid of any bacterial clusters (microcolonies) on the apatitic surface, while the *in situ* pH values at the biofilm-apatite interface were nearly one unit higher in arginine-treated biofilms (versus the vehicle control). Our data reveal new biological properties of L-arginine that impact biofilm matrix assembly and the dynamic microbial interactions associated with pathogenic biofilm development, indicating the multiaction potency of this promising biofilm disruptor.

IMPORTANCE

Dental caries is one of the most prevalent and costly infectious diseases worldwide, caused by a biofilm formed on tooth surfaces. Novel strategies that compromise the ability of virulent species to assemble and maintain pathogenic biofilms could be an effective alternative to conventional antimicrobials that indiscriminately kill other oral species, including commensal bacteria. L-Arginine at 1.5% has been shown to be clinically effective in modulating cariogenic biofilms via alkali production by arginolytic bacteria. Using a mixed-species ecological model, we show new mechanisms by which L-arginine disrupts the process of biofilm matrix assembly and the dynamic microbial interactions that are associated with cariogenic biofilm development, without impacting the bacterial viability. These results may aid in the development of enhanced methods to control biofilms using L-arginine.

Biofilms formed on surfaces are highly organized and structured microbial communities enmeshed in an extracellular matrix composed of polymeric substances, such as exopolysaccharides (EPS) (1, 2). Many human infections are caused and/or exacerbated by virulent biofilms, including those occurring in the mouth (3). Among them, dental caries is one of the most prevalent and costly biofilm-dependent infectious diseases worldwide (4). The assembly of caries-producing (cariogenic) biofilms on saliva-coated teeth is a prime example of the consequences arising from interactions between bacteria (and their products) and diet (e.g., sugars) that promotes microbial accumulation as an EPS-rich matrix develops (5). EPS are key matrix components that act as a supportive three-dimensional (3D) scaffold and barrier to diffusion, modulating growth of and providing protection to pathogens (1, 2, 6). A major challenge in biofilm-related diseases is that the embedded bacteria become recalcitrant to antimicrobials, making them difficult to remove without disturbing the normal flora.

In the mouth, a highly diverse microbial community is constantly interacting with the salivary pellicle present on the tooth surface, to which early colonizers, including viridans group streptococci and *Actinomyces* spp., can adhere and coadhere with other organisms (7, 8). Cariogenic bacteria, such as *Streptococcus mutans*, can be also present in this initial colonizing community, although in varied numbers, which is dependent on the host diet

Received 16 January 2016 **Accepted** 1 May 2016

Accepted manuscript posted online 9 May 2016

Citation He J, Hwang G, Liu Y, Gao L, Kilpatrick-Liverman L, Santarpia P, Zhou X, Koo H. 2016. L-Arginine modifies the exopolysaccharide matrix and thwarts *Streptococcus mutans* outgrowth within mixed-species oral biofilms. J Bacteriol 198:2651–2661. doi:10.1128/JB.00021-16.

Editor: G. A. O'Toole, Geisel School of Medicine at Dartmouth

Address correspondence to Hyun Koo, koohy@dental.upenn.edu.

Supplemental material for this article may be found at http://dx.doi.org/10.1128/JB.00021-16.

(9). However, environmental changes, such as frequent sucrose intake, can serve as the catalyst for cariogenic biofilm formation, since this sugar serves as a substrate for the production of both EPS and acids (5). *S. mutans* can rapidly orchestrate the assembly of virulent biofilm via EPS synthesis by exoenzymes (e.g., glucosyltransferases) bound on the pellicle and on bacterial surfaces (10–12). The EPS formed *in situ* enhances the local accumulation of bacteria on teeth via glucan-binding mechanisms while enmeshing them in a diffusion-limiting matrix (2, 10, 13–15). This ultimately creates highly adherent and cohesive biofilm architecture that shelters and protects resident organisms (2, 6, 14–16). In parallel, sugars are fermented by bacteria within biofilms, creating acidic microenvironments. The low-pH niches induce EPS synthesis and cause ecological shifts by favoring the growth of acidogenic and acid-tolerant bacteria. Consequently, local acidity ensures cariogenic biofilm accretion and acid dissolution of the adjacent enamel, leading to the onset of caries (17). Thus, novel strategies that compromise the ability of virulent species to assemble and maintain pathogenic biofilms could be alternatives to conventional broad-spectrum antimicrobials, which can indiscriminately kill other oral species, including commensal bacteria.

L-Arginine has been shown to potentially modulate cariogenic biofilms. In the oral cavity, arginine, mainly derived from diet and host saliva, is utilized by arginolytic bacteria (e.g., *S. gordonii*) via the arginine deiminase system (ADS) with end products, such as ammonia (18). Due to the pH raising effect of ammonia, arginine has been regarded as a potential endogenous caries modulator (18–21). Indeed, the levels of free arginine in the saliva of caries-free individuals were significantly higher than those in the saliva of those with caries (22), and a positive correlation between ADS activity in plaque biofilms and absence of caries has been clinically validated in adults (23) and children (24). These findings suggest the possibility of arginine supplementation as a strategy to disrupt pathogenic biofilms. *In vitro* studies show that exogenous L-arginine can inhibit the adhesion of *S. mutans* to saliva-coated surfaces (25), influence single-species *S. gordonii* biofilm formation (26), and destabilize a saliva-derived biofilm community (27). Arginine treatments also increased *arcA* gene (involved in arginine metabolism) abundance compared to that in untreated biofilms, indicating a potential role for the enrichment of alkali-producing microflora (28).

The available laboratory and clinical evidence supports exogenous L-arginine supplementation at the concentration of 1.5% (wt/vol) as a feasible adjunctive anticaries approach via ADS activity (28–31). However, L-arginine may inflict additional changes in the biofilm milieu under conditions conducive to dental caries. Here, we provide new insights on how topical L-arginine exposure modulates biofilm development using a mixed-species model containing both cariogenic (*S. mutans*) and arginolytic (*S. gordonii*) bacteria under sucrose challenge. We found that L-arginine thwarts *S. mutans* outgrowth and promotes *S. gordonii* dominance while maintaining *A. naeslundii* growth within sucrose-grown biofilms. Interestingly, L-arginine represses *S. mutans* genes associated with insoluble EPS (*gtfB*) and bacteriocin (*SMU.150*) production during early biofilm stages. In contrast, *spxB* expression by *S. gordonii* increases sharply at later phases of development, resulting in elevated levels of H_2O_2 in arginine-treated biofilms. Together, these effects caused major disruption in the EPS matrix assembly, 3D biofilm architecture, and *in situ* pH at the biofilm-apatite interface. Our data reveal intriguing and dynamic multifaceted roles of L-arginine as a potent disruptor of both EPS matrix and microbial interactions that are associated with cariogenic biofilm development.

MATERIALS AND METHODS

Bacterial strains and mixed-species ecological biofilm model. *S. mutans* UA159 serotype c (ATCC 700610), *A. naeslundii* ATCC 12104, and *S. gordonii* DL1 were used in present study. These three strains were selected because *S. mutans* is a well-established virulent cariogenic bacterium (32). *S. gordonii*, a pioneer colonizer of dental biofilm, is arginolytic and ADS positive (33), and *A. naeslundii* is also detected during the early stages of dental biofilm formation (34). Furthermore, *S. mutans* UA159 and *S. gordonii* DL1 have been used in multiple laboratories in several *in vitro* biofilm models, and they are the strain of choice for *in vivo* (rodent) models of dental caries (35–39). Finally, these strains are well characterized (both genetically and phenotypically) and standardized, which are critical for the reproducibility of the study. All strains were stored at −80°C in tryptic soy broth containing 20% glycerol.

The biofilm method used in this study was designed to mimic the formation of cariogenic biofilms according to the "ecological plaque" concept, as detailed previously (6, 40, 41). Briefly, hydroxyapatite discs (1.25 cm in diameter, surface area of 2.7 ± 0.2 cm^2; Clarkson Chromatography Products, Inc., South Williamsport, PA) were coated with filter-sterilized clarified human whole saliva (sHA) (6, 40). *S. mutans* UA159, *A. naeslundii* ATCC 12104, and *S. gordonii* DL1 were grown in ultrafiltered (10-kDa molecular mass cutoff membrane; Prep/Scale, Millipore, MA) buffered tryptone-yeast extract broth (UFTYE; 2.5% tryptone and 1.5% yeast extract [pH 7.0]) with 1% glucose to mid-exponential phase (37°C, 5% CO_2). Each of the bacterial suspensions was then mixed to provide an inoculum with a defined microbial population of *S. mutans* (10^4 CFU/ml), *S. gordonii* (10^4 CFU/ml), and *A. naeslundii* (10^6 CFU/ml). To promote the ecological changes found under cariogenic conditions, we determined that the selected inoculum can promote the microbial shifts that favor *S. mutans* dominance following the addition of 1% sucrose in a reproducible manner, both in terms of timing of the changes and the number of CFU. The mixed population was inoculated in 2.8 ml of UFTYE containing 0.1% (wt/vol) sucrose and incubated for 19 h to form an initial biofilm community on the sHA surface. The biofilms were transferred to UFTYE containing 1% sucrose to induce environmental changes to simulate a cariogenic challenge from 29 h. The culture medium was changed twice daily (8 a.m. and 6 p.m.) until the end of the experimental period (115 h) (Fig. 1).

Biofilm treatments. Biofilm treatments started at 19 h and were carried out at 8 a.m., 1 p.m., and 6 p.m. each day, as detailed in Fig. 1. Free L-arginine (Ajinomoto AminoScience LLC, Raleigh, NC) was prepared at concentrations of 0.75%, 1.5%, and 3% (wt/vol) in filter-sterilized aqueous solution, and the pH was adjusted to 8 to 8.5 using phosphoric acid to be congruent with the pH values in arginine-containing formulations (29). Before treatment, biofilms were dip-washed in 2.8 ml of sterile saline solution (0.89% [wt/vol] NaCl) and then transferred into 2.8 ml of 0.75%, 1.5%, and 3% L-arginine or vehicle control (filter-sterilized water with pH adjusted to 8 to 8.5 using NaOH) for 10 min. The discs were shaken to remove excess and then transferred into wells containing culture medium without wash. All the discs were inoculated to assess the biological effects of L-arginine at the specific time points (Fig. 1).

Bacterial cell viability, biomass, and exopolysaccharide assays. At selected time points (29, 53, 67, 91, and 115 h), biofilms were removed, homogenized via sonication, and subjected to biochemical and microbiological analyses, as detailed previously (6, 40, 42); our sonication procedure does not kill bacterial cells while providing optimum dispersal and maximum recoverable counts. Aliquots of biofilm suspension were serially diluted and plated on blood agar using an automated Eddy Jet Spiral Plater (IUL, SA, Barcelona, Spain). The three species were differentiated by observation of colony morphology combined with microscopic examination of cells from selected colonies, and the total number of viable cells

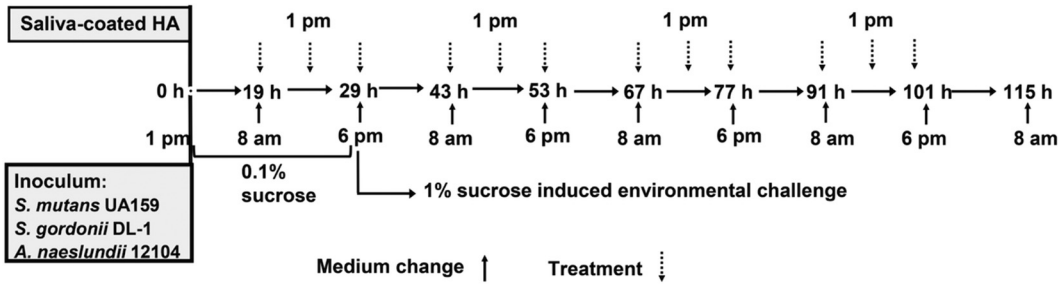

FIG 1 Biofilm preparation and treatment regimen. The inoculum with a defined microbial population of *S. mutans* (10^4 CFU/ml), *S. gordonii* (10^4 CFU/ml), and *A. naeslundii* (10^6 CFU/ml) was inoculated in 2.8 ml of UFTYE containing 0.1% (wt/vol) sucrose (0 h) and cultured without disturbance during the first 19 h to form an initial biofilm community on the sHA surface. The biofilms were transferred to UFTYE containing 1% sucrose to induce environmental changes simulating a cariogenic challenge from 29 h. The culture medium was changed twice daily (8 a.m. and 6 p.m.) until the end of the experimental period. Biofilm treatments started at 19 h and were carried out at 8 a.m., 1 p.m., and 6 p.m. each day.

in each of the biofilms was determined by counting CFU (6, 40). The remaining suspension was centrifuged at 5,500 × *g* for 10 min at 4°C, and the cell pellet was washed twice with water, dried in the dry oven at 105°C for 24 h, and weighed (43). The water soluble EPS (s-EPS), insoluble exopolysaccharides (i-EPS), and intracellular iodophilic polysaccharides (IPS) were extracted and quantified via colorimetric assays (42–44). Furthermore, the pH of the culture medium of treated and untreated biofilms was monitored every 2 h with an Orion pH electrode attached to an Orion 290 A+ pH meter (Thermo Fisher Scientific).

Three-dimensional confocal imaging of biofilms. The influence of arginine exposure on the 3D biofilm architecture and the spatial distribution of EPS and bacterial biomass within intact biofilms were assessed using our established protocols optimized for confocal biofilm imaging and quantification (6, 40). Briefly, EPS was labeled using 2.5 μM Alexa Fluor 647-labeled dextran conjugate (10 kDa, 647/668 nm; Molecular Probes, Inc., Eugene, OR), while the microbial cells were stained with 2.5 μM SYTO 9 (485/498 nm; Molecular Probes, Inc.) (6). Laser scanning confocal fluorescence imaging of 67-h biofilms was obtained with an Olympus FV 1000 two-photon laser scanning microscope (Olympus, Tokyo, Japan) equipped with a 20× (0.45 numerical aperture) water immersion objective lens. The confocal image series were generated by optical sectioning at each selected position, and the step size of z-series scanning was 2 μm. The confocal images were analyzed via COMSTAT for the quantification of EPS and bacteria within intact biofilms, while the Amira 5.4.1 software (Visage Imaging, San Diego, CA) was used to create 3D renderings of the biofilm architecture (6, 40).

***In situ* pH measurement.** To measure the *in situ* biofilm pH, we used fluorescent pH indicator LysoSensor yellow/blue (Molecular Probes, Inc.) labeling method, as described previously (6). Briefly, the 67-h biofilms were incubated with LysoSensor yellow/blue-labeled dextran conjugate, and the pH values within intact biofilms were measured based on fluorescence intensity ratios of the dual-wavelength fluorophore. The fluorophore exhibits a dual-emission spectral peak (fluorescence emission maxima, 452 nm and 521 nm), and the ratio between the fluorescence intensity of these two spectral peak is pH dependent within biofilms (6). The fluorescence intensity of both emission wavelengths and the ratio of fluorescent intensity (I_{450}/I_{520}) within each biofilm image were measured using Image J 1.44 and its calculation tools (http://rsbweb.nih.gov/ij/download.html). The ratios of fluorescence intensity of selected areas within each biofilm image were converted to pH values using the titration curves of ratios versus pH (ranging from 3.5 to 7.0), as detailed previously (6).

RNA isolation and real-time analysis. Quantitative reverse transcription-PCR (qRT-PCR) was performed to quantify the expression of specific target genes (*gtfB* and *SMU.150* of *S. mutans*, and *spxB* and *arcA* of *S. gordonii*). Biofilms were harvested immediately after arginine exposure (at 43 h and 53 h) and 4 h after treatment (at 33 h and 47 h) from the same initial inoculum (Fig. 1; also see "Biofilm treatments," above). RNA was extracted and purified from biofilms using standard protocols optimized for biofilms (42). The RNA integrity numbers (RIN) of purified samples used for qRT-PCR were determined by microcapillary electrophoresis on an Agilent 2100 Bioanalyzer (Agilent Technologies, Santa Clara, CA). The cDNA was synthesized from 1 μg of purified RNA (RIN, ≥9) with the Bio-Rad iScript cDNA synthesis kit (Bio-Rad Laboratories, Inc., Hercules, CA), and quantitative amplification conditions using Bio-Rad iTaq Universal SYBR green Supermix and Bio-Rad CFX96 system (Bio-Rad Laboratories, Inc.). The primers used in present study were listed in Table 1. Standard curves for each primer were used to determine the relative number of cDNA molecules, and relative expression was calculated by normalizing to the 16S rRNA gene transcripts (6). The Minimum Information for Publication of Quantitative Real-Time PCR Experiments (MIQE) guidelines were used for quality control of the data generated and for data analysis.

H_2O_2 concentration measurement. The concentration of H_2O_2 was measured using a horseradish peroxidase (HRP) enzymatic assay (45). Briefly, biofilm was gently washed once, released into glass tubes containing 0.5 ml of reaction mixture (1 mg/ml 3,3′,5,5′-tetramethylbenzidine [TMB] and 1:2,000 dilution of HRP [Invitrogen] in 0.1 M sodium acetate buffer [pH 4.5]), and incubated at room temperature for 15 min. The same volume of H_2SO_4 (2 N, 0.5 ml) was added into tubes for reaction termination. The supernatant was transferred into Eppendorf tubes, centrifuged at 4°C for 1 min, and the absorbance at 450 nm was determined using a plate reader. To determine the concentration of H_2O_2, a standard curve was prepared using a serially diluted H_2O_2 solution, and the data were normalized with dry weight.

Statistical analysis. The data are presented as the mean ± one standard deviation (SD). Each of the experiments was repeated at least 3 times. Pairwise comparisons were made between the test and control using Student's *t* test. The chosen level of significance for all statistical tests in present study was a *P* value of <0.05.

RESULTS

L-Arginine topical exposure causes microbial shifts preventing *S. mutans* outgrowth and favoring *S. gordonii* survival. We first assessed the influence of L-arginine on the dynamics of microbial population changes within biofilms. The treatment regimen is shown in Fig. 1, and three concentrations (0.75%, 1.5%, and 3%) were tested. As shown in Fig. 2, the introduction of L-arginine caused dramatic changes in the number and proportion (right panels) of viable microbial populations (versus vehicle control). In vehicle-treated biofilms, *S. mutans* was the dominant species at 29 h and maintained its dominance to the endpoint (115 h), consistent with a recent *in vivo* study showing that *S. mutans* outcompetes *S. gordonii* in a rodent caries model (39). *S. mutans* was

TABLE 1 Primers used for qRT-PCR in the present study

Primer target	Direction[a]	Primer sequence
S. gordonii 16S rRNA	F	5′-GCTTGCTACACCATAGACTG-3′
	R	5′-AGCCGTTACCTCACCTAC-3′
S. mutans 16S rRNA	F	5′-ACCAGAAAGGGACGGCTAAC-3′
	R	5′-TAGCCTTTTACTCCAGACTTTCCTG-3′
gtfB	F	5′-AGCAATGCAGCCAATCTACAAAT-3′
	R	5′-ACGAACTTTGCCGTTATTGTCA-3′
SMU.150	F	5′-GAAGGTATCGGGTGGAGAAG-3′
	R	5′-CCCAAGTGCCTACACAATATG-3′
spxB	F	5′-GCGTACATCTCCACTCTTTG-3′
	R	5′-CACCCATGATGTTCCATACTT-3′
arcA	F	5′-GTCTTTGACCTCACCAGAAA-3′
	R	5′-ACTCACGAATAGCCACTTTAG-3′

[a] F, forward; R, reverse.

considered the dominant species based on its higher proportion of viable cells relative to others (Fig. 2A, right). In parallel, the viable population of *S. gordonii* declined, while *A. naeslundii* was undetectable after 67 h of biofilm development.

In contrast, 1.5% or 3% L-arginine exposure shifted the microbial populations from *S. mutans* dominance (at 29 h) to *S. gordonii*-dominated biofilm between 53 h and 67 h, which were also characterized by detectable levels of *A. naeslundii* throughout the experimental period. Although the total CFU counts in 1.5% L-arginine-treated biofilms appear similar at 53 h (as the values are in log scale), the proportions of viable *S. mutans* and *S. gordonii* cells start to shift at this time point, which becomes more evident at 67 h. This observation indicates that L-arginine requires some time to exert its effects (at least in part via metabolism by arginolytic bacteria, e.g., *S. gordonii*) and thereby impact the microbial composition. Furthermore, the proportion of *S. mutans* viable cells population declined sharply in L-arginine-treated biofilms, although this bacterium was able to survive over time; 0.75% L-arginine showed limited effects on the microbial composition compared to vehicle control or higher concentrations of L-arginine. Interestingly, we observed an overall drop in the total number of cells between 53 h and 67 h, particularly in the vehicle control group. The exact reasons are unclear, but it is possible that some of the biofilm detached due to increased biomass accumulation, followed by further regrowth after this time point.

Clearly, L-arginine at 1.5% or 3% (despite brief topical exposures) is capable of inducing major changes in the viable microbial populations and proportions despite the presence of sucrose (a cariogenic stimuli), promoting the transition from a virulent (high levels of *S. mutans* and small numbers of *S. gordonii*) to a potentially less-cariogenic (*S. gordonii* dominated) biofilm. The total viable bacterial cell population in the biofilm was unaffected by L-arginine treatments.

L-Arginine treatments impact the biomass accumulation, polysaccharide content, and 3D architecture of biofilms. Concomitantly, we also observed that the biomass (dry weight) of the 1.5% and 3% L-arginine-treated biofilms was greatly decreased compared to that of vehicle-treated biofilms at each of the time points of biofilm development (Fig. 3A). It is possible that the reduced biomass is associated with changes in EPS content, as fewer *S. mutans* cells are present in the L-arginine-treated biofilms. *S. mutans* produces large amounts of insoluble glucans in the presence of sucrose, forming a matrix that provides bulk and structural integrity to the biofilm while facilitating the creation of localized acidic microenvironments (10). Indeed, the total amount of insoluble EPS in 1.5% and 3% arginine-treated biofilms (115 h) was reduced by ~3-fold compared to those treated with vehicle (Fig. 3B). Consistent with the microbiological data, 1.5% or 3% L-arginine treatments were equally effective in reducing both the biofilm biomass (dry weight) and the amount of insoluble EPS (versus vehicle control), while the biological effects of 0.75% L-arginine were modest. Based on these findings, we selected 1.5% L-arginine, which has also been shown to be a clinically effective concentration (29–31), for further analyses. Interestingly, the content of soluble EPS and intracellular polysaccharides (IPS) was unaffected (see Fig. S1 in the supplemental material) (despite the reduction of *S. mutans*), likely due to an increase in the number of *S. gordonii* cells, which is capable of synthesizing soluble glucans from sucrose, and to produce and store IPS.

Confocal images showed clear alteration in the biofilm 3D architecture by 1.5% L-arginine treatments, showing a defective EPS matrix and areas devoid of bacterial clusters or microcolonies on the sHA surface (Fig. 4). In contrast, vehicle-treated biofilm contains a well-structured EPS matrix, with bacterial clusters covering the entire apatitic surface. Furthermore, the spatial distribution of EPS and bacteria across the biofilm thickness (see selected area in the merged images, Fig. 4) was also compromised in arginine-treated biofilms (versus vehicle control). Although the confocal images show overall less bacterial biomass in arginine-treated biofilms, it is noteworthy that several densely packed microcolonies are still present. Collectively, the data show that topical applications of exogenous L-arginine at a concentration of 1.5% cause major biochemical and structural changes, as *S. mutans* outgrowth was suppressed while *S. gordonii* dominance was promoted within treated biofilms.

***S. mutans* and *S. gordonii* gene expression profile following L-arginine treatment.** To further understand the interplay between *S. mutans* and *S. gordonii* during biofilm development and

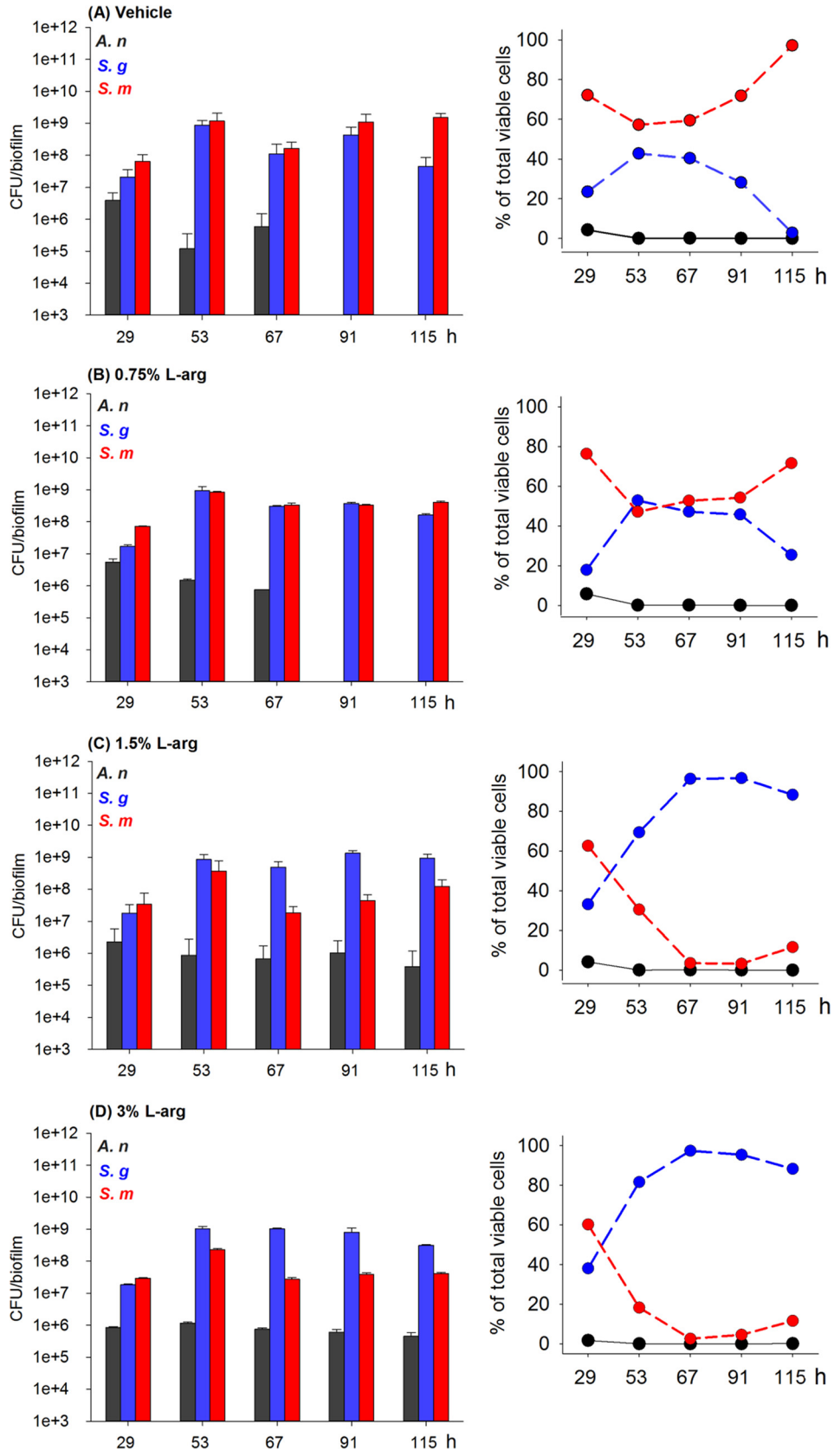

FIG 2 Dynamic changes of microbial composition of biofilms with and without topical L-arginine (L-arg) exposure. Total viable cells for each experimental group are shown as bar graphs, while the proportion of different bacterial species in the treated biofilms is presented in the right graphs ($n = 12$). In vehicle-treated biofilms, *S. mutans* (*S. m*) was the dominant species from 29 h to the endpoint, and the viable population of *S. gordonii* (*S. g*) declined while *A. naeslundii* (*A. n*) was undetectable after 67 h. In contrast, 1.5% and 3% L-arginine-treated biofilms were characterized by *S. gordonii* dominance from 53 h and detectable levels of *A. naeslundii* throughout the experimental period, while the *S. mutans* viable population sharply declined. L-Arginine at 0.75% showed modest effects on the microbial composition compared to vehicle control or the higher concentrations of L-arginine.

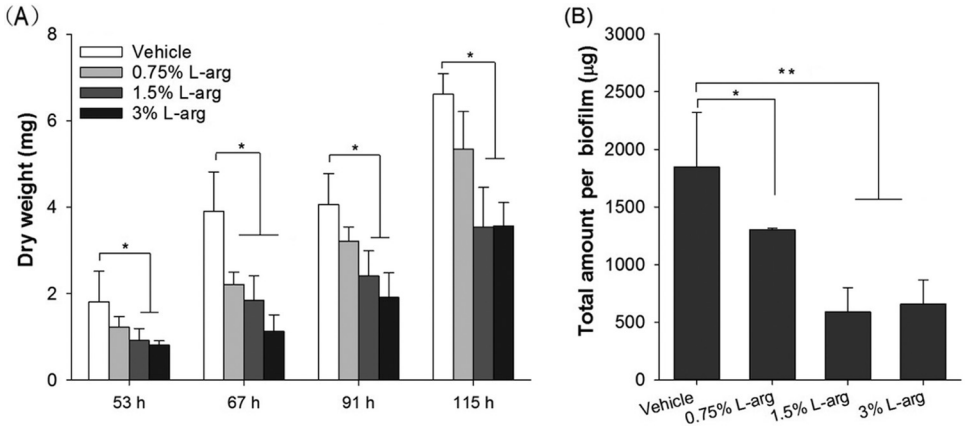

FIG 3 Biomass and insoluble exopolysaccharide composition of biofilms with and without L-arginine exposure. Shown are dry weight (A) and total amounts (B) of insoluble exopolysaccharides ($n = 9$). The biomass (dry weight) of the 1.5% and 3% L-arginine-treated biofilms was greatly reduced compared to vehicle-treated biofilms at each of the time points. Water-insoluble EPS in arginine-treated biofilms (115 h) was reduced by ~3-fold compared to those treated with vehicle control; 0.75% L-arginine showed limited biological effects. Values are significantly different from each other at $P < 0.05$ (*) and $P < 0.01$ (**).

L-arginine exposure, we examined the expression pattern of specific genes associated with insoluble EPS matrix assembly (*gtfB* of *S. mutans*), interspecies interactions (*SMU.150* of *S. mutans* and *spxB* of *S. gordonii*), and arginine metabolism (*arcA* of *S. gordonii*). The dynamics of gene expression (normalized by 16S rRNA) were analyzed between 29 h and 53 h, because the microbial composition shift occurred during this period; 29-h biofilms were excluded since we could not obtain sufficient biomass for RNA extraction.

The transcription of *gtfB* by *S. mutans* was significantly re-

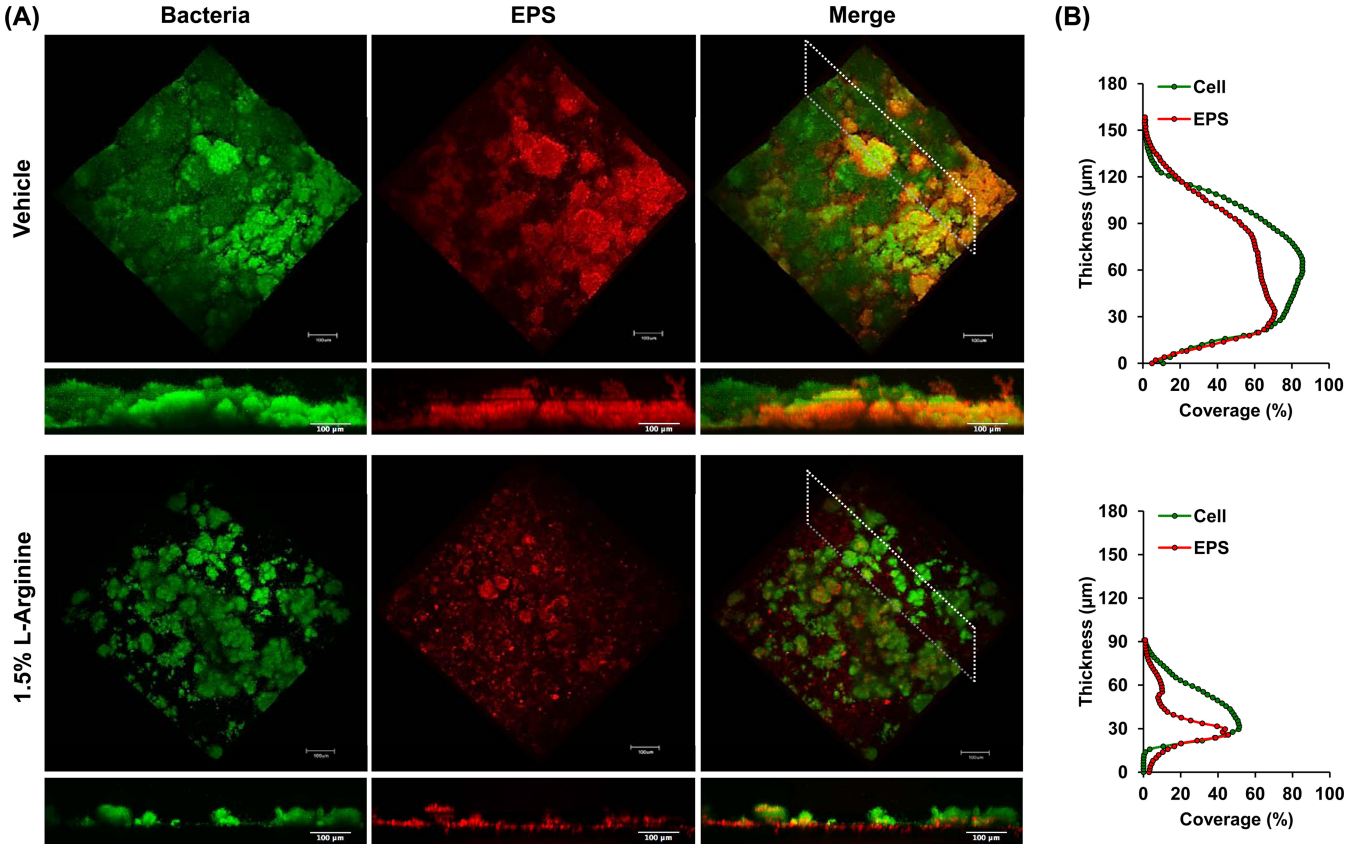

FIG 4 Three-dimensional architecture of biofilms with and without 1.5% L-arginine exposure. (A) Representative 3D rendering of 67-h biofilms treated with vehicle control or 1.5% L-arginine. (B) The EPS/cell distribution across the biofilm thickness at the selected area in the merged image in panel A was determined via COMSTAT. A defective EPS matrix and areas devoid of bacterial clusters or microcolonies on the sHA surface were observed in the arginine-treated biofilms. In contrast, vehicle-treated biofilms show a well-structured EPS matrix with bacterial clusters covering the entire apatitic surface.

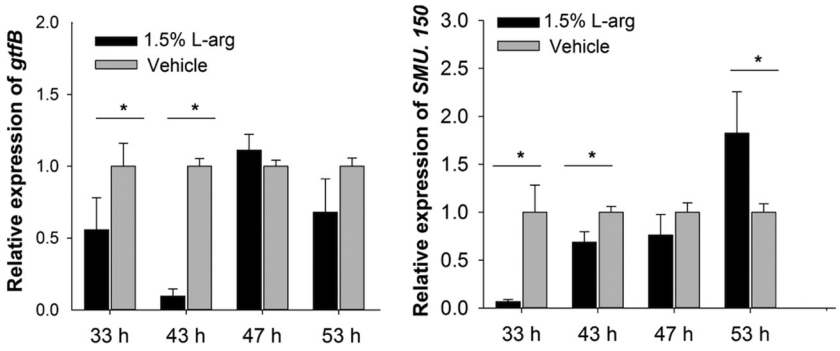

FIG 5 L-Arginine (1.5%) exposure disrupts the dynamics of gene expression of *S. mutans* associated with EPS and bacteriocin ($n = 6$). *SMU.150* and *gtfB* gene expression by *S. mutans* decreased in arginine-treated biofilm at early time points (33 h and 43 h), but *SMU.150* expression increased at 53 h. Values are significantly different from each other at $P < 0.05$ (*).

pressed by 1.5% L-arginine exposure at early time points (33 h and 43 h) (Fig. 5), which agrees well with the biochemical and structural data. GtfB is essential for both *S. mutans* accumulation and EPS-rich matrix development (10). Furthermore, we observed interesting changes in the expression pattern of genes involved in the competitive interactions between *S. mutans* and *S. gordonii*. *SMU.150* gene expression by *S. mutans* was severely repressed in arginine-treated biofilm at an early time point (33 h) and to a lesser extent at 43 h, while it was moderately increased at 53 h (Fig. 5). Intriguingly, *S. gordonii spxB* transcripts sharply increased (>3.5-fold versus vehicle control) at a later time point (53 h) (Fig. 6). *SMU.150* is involved in the synthesis of bacteriocin that is capable of inhibiting the growth of non-*mutans* streptococci (46–48). Conversely, pyruvate oxidase encoded by *spxB* is largely responsible for H_2O_2 production (47), which can be used by *S. gordonii* to outcompete *S. mutans* within mixed-species biofilms (47). To further explore if the levels of H_2O_2 were increased in biofilms treated with L-arginine, we measured the amounts of hydrogen peroxide in the whole biofilms via a colorimetric assay (49). Consistent with the *spxB* expression profile, a higher H_2O_2 level was found in 53-h biofilms treated with arginine versus vehicle control (Fig. 6).

In the oral cavity, arginine is primarily metabolized through the ADS system (18). The genes encoding the ADS are commonly arranged in an operon, and the *arcA* gene encodes arginine deiminase, a key component of ADS system, which hydrolyzes arginine to generate citrulline and ammonia (19). The expression of *arcA* was slightly increased, albeit the differences were not statistically significant (see Fig. S2 in the supplemental material); it is possible that strongly arginolytic organisms, such as *S. gordonii*, do not respond to elevated concentrations of arginine to induce *arcA* expression. Altogether, topical exposure to 1.5% L-arginine is capable of modulating streptococcal competition by downregulating *gtfB* and *SMU.150* and enhancing *spxB* expression, which might explain at least in part the biochemical and microbiological changes within treated biofilms.

***In situ* pH at the biofilm-sHA interface increases following L-arginine treatment.** The deleterious effects of arginine exposure on *S. mutans* accumulation, insoluble EPS content, and matrix assembly combined with enhancement of *S. gordonii* growth might affect the pH at the surface of biofilm attachment, which is the hallmark for caries initiation (50, 51). Previous studies have shown the pH-raising capacity of arginine by measuring the pH of the surrounding culture medium (52) or via electrodes placed in the biofilm (28). However, *in situ* pH measurements at the sHA-

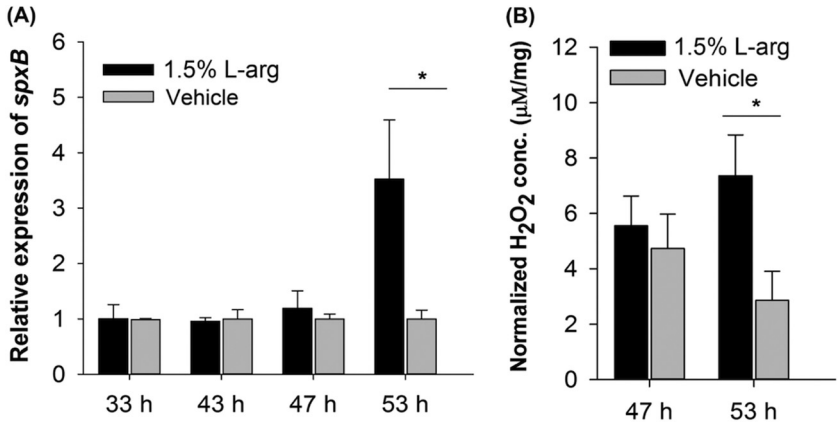

FIG 6 L-Arginine (1.5%) exposure promotes H_2O_2 production by *S. gordonii*. Expression of *S. gordonii spxB* ($n = 6$) (A) and H_2O_2 amounts ($n = 12$) (B) in the treated biofilms were determined. *S. gordonii spxB* transcripts sharply increased (>3.5-fold versus vehicle control) at a later time point (53 h), and a higher H_2O_2 level was found in 53-h biofilms treated with arginine (versus vehicle control). Values are significantly different from each other at $P < 0.05$ (*). conc., concentration.

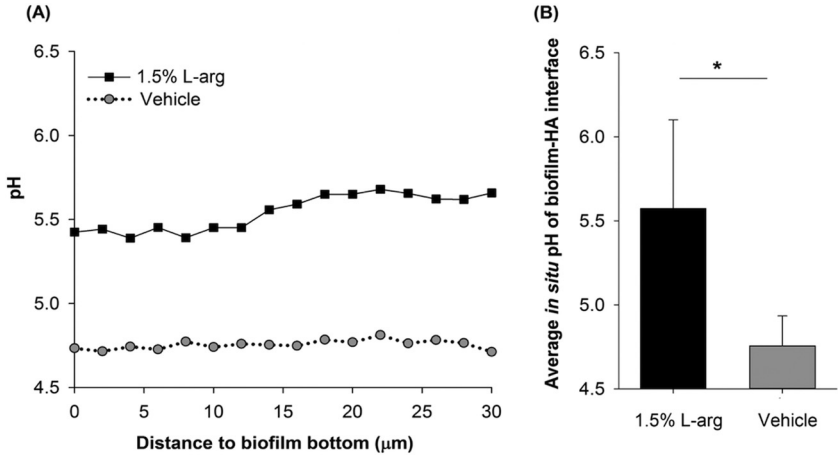

FIG 7 *In situ* pH measurement at the biofilm-apatite interface. *In situ* pH values in 67-h biofilm were determined every 2 μm from the sHA surface (A) and averaged based on pH measurements across the biofilm interface ($n = 50$) (B). The differences in the *in situ* pH values were as high as one full unit (versus vehicle-treated biofilms), particularly between 20 to 30 μm from the sHA surface. Values are significantly different from each other at $P < 0.05$ (*).

biofilm interface without disrupting the integrity of the biofilm 3D architecture have not been reported yet.

Recently, we devised a noninvasive pH mapping approach using a fluorescent pH indicator to determine pH values throughout intact biofilm structure (6). Here, we focused on measuring the pH values in close proximity of the sHA surface (up to 30 μm from the surface), because the maintenance of acidic pH at the biofilm-sHA interface promotes demineralization of the adjacent apatite (50, 51); the critical pH for demineralization of enamel appears to be as low as 5.1 in the plaque fluid, as recently reviewed (51). We found that the average pH values of 1.5% L-arginine-treated biofilms were significantly higher than those from vehicle-treated biofilms (Fig. 7). Strikingly, the differences in the *in situ* pH values were as high as one full unit (versus vehicle-treated biofilms), particularly between 20 and 30 μm from the sHA surface (Fig. 7A), with pH above 5.7, which might impact the initiation and progression of carious lesions.

DISCUSSION

The favorable modification of the microbial composition by L-arginine mediated via ADS activity has been recognized as the primary anticaries mechanism (18, 29), since ADS could generate alkali from arginine to neutralize excessive acid within plaque. Here, we established a mixed-species biofilm model to explore additional mechanisms by which L-arginine impacts the cariogenic properties of biofilms. Although our model does not simulate the episodic dietary intake in humans, it does mimic sucrose-rich exposure conditions found in high caries-active individuals, as well as the biochemical and microbiological changes associated with cariogenic biofilm formation (4, 5). Our data reveal that topical applications of 1.5% L-arginine similar to multiple daily oral exposures disrupt insoluble EPS production, which impairs *S. mutans* accumulation and further biofilm build-up. At the same time, it modulates interspecies competition that favors *S. gordonii* growth and dominance. These modifications in turn result in defective EPS matrix assembly, altered biofilm 3D architecture, and significantly higher pH at the biofilm-apatite interface that could attenuate biofilm virulence (cariogenicity) without bacterial killing (53).

Considering the essential roles of EPS in the development and cariogenicity of oral biofilms (1–3, 10), we propose that the action of L-arginine as a disruptor of the process of biofilm matrix assembly is an important additional mechanism for its caries-protective effect. Our data suggest that the repression of *gtfB* expression at early stages of biofilm formation combined with a rapid decline in the proportion of *S. mutans* (and its lower abundance during the later stages of biofilm development) might explain the impairment of the EPS matrix assembly over time. Insoluble EPS (glucans) produced by GtfB promote selective binding and accumulation of *S. mutans* onto apatitic surfaces (10–12). Furthermore, it also enhances cell clustering and microcolony development that facilitate *S. mutans* persistence within biofilms (2, 6, 13, 16). Thus, the disruption of GtfB-derived EPS would markedly impact the ability of *S. mutans* to colonize and accumulate within biofilms. As the main producer of insoluble EPS within the oral microbiome (2), such effects could sharply reduce the assembly of the biofilm matrix as well as the biofilm bulk and biomass, as observed in the arginine-treated biofilms.

The highly insoluble nature of GtfB-derived glucans is also essential for the scaffolding and structural integrity of the biofilm 3D architecture (1, 2, 6, 16), which directly modulates the surface attachment strength of the biofilm (54). Interestingly, L-arginine appears to affect the biomechanical properties of *S. mutans*-derived EPS, which attenuated the biofilm adhesion strength (25). In addition to providing bulk and mechanical stability, the EPS matrix also forms a diffusion-limiting milieu that embeds cariogenic bacteria, forming protective niches against antimicrobials (1, 6, 55). Recently, it was shown that the antimicrobial efficacy of cetylpyridinium chloride (CPC) against oral biofilms was enhanced when used in combination with arginine *in vitro* (27). The authors suggested potential alterations in the EPS matrix, which could facilitate CPC penetration (27); our data certainly support this clinically relevant observation. It is readily apparent that L-arginine effects on EPS might suppress biofilm accumulation while making them more susceptible to treatment or removal.

The results from this study also show that topical exposure of L-arginine affects key modulators involved in competitive interspecies interactions between *S. mutans* and *S. gordonii*. The ex-

pression of *S. mutans SMU.150*, which encodes mutacin, was repressed during the early biofilm development stage. Mutacin production by *S. mutans* is known to inhibit the growth of commensal bacteria, such as *S. gordonii* (46). Conversely, L-arginine exposure induced *S. gordonii* H_2O_2 production, which is an effective "chemical weapon" against *S. mutans* growth *in vitro* (47). Interestingly, the expression of the mutacin-encoding gene by *S. mutans* and *spxB* by *S. gordonii* are both higher in the arginine-treated biofilms at the later time point. It is possible that *S. mutans* is upregulating mutacin production in response to H_2O_2 stress caused by the growing numbers of *S. gordonii* actively expressing *spxB* in the arginine-treated biofilms, which in turn would help *S. mutans* persist in this unfavorable milieu. This observation might explain, at least in part, why *S. mutans* cells are not completely eliminated and survive in the biofilm.

A. naeslundii also benefits from L-arginine supplementation, as this bacterium is detected throughout the experiment period in arginine-treated biofilms while absent after 67 h in control biofilms. Since *A. naeslundii* has been reported to interact with *S. gordonii* and promote its growth (56), the enhanced *A. naeslundii* survival in arginine-treated biofilms may indirectly help *S. gordonii* compete against *S. mutans*. Thus, arginine is capable not only of hindering *S. mutans* colonization and initial accumulation via disruption of EPS-mediated mechanisms but also the competitiveness of this pathogen within sucrose-grown biofilms (although *S. mutans* appears to survive and possibly fight back over time). We propose that arginine might play an active role in mediating the regulatory pathways associated with the transcription of *gtfB*, *SMU.150*, and *spxB*. Future studies shall elucidate the underlying molecular mechanisms regulating the expression of these genes and their dynamic interactions. It should be noted that the regulation of these genes is complex and linked with multiple pathways, which may reveal additional therapeutic targets.

Ammonia generation via ADS activity can neutralize glycolytic acids and modulate pH homeostasis within biofilms (18). Our data reveal that defective assembly of EPS matrix and microcolony formation as a result of L-arginine exposure may also contribute to elevated *in situ* pH at the biofilm-sHA interface. Previous studies have shown that EPS-enmeshed microcolonies could trap acid at the sHA surface and/or restrict the access of neutralizing buffer to generate acidic microenvironments locally due to metabolic activity of the densely packed bacteria enmeshed within a diffusion-limiting EPS matrix, particularly at the deeper layers of the biofilm (6, 57, 58). Altogether, it appears that the combination of ADS activity and favorable ecological changes with disruption of EPS/microcolony development may offer a more comprehensive explanation for the biofilm pH-related effects associated with L-arginine exposure. However, additional studies are needed to further understand the role of protonated/deprotonated forms of L-arginine (which varies with pH) in biofilm formation and virulence and validate the biological effects observed here using *in vivo* and longitudinal clinical studies.

In conclusion, our data reveal intriguing new biological insights into how L-arginine impacts the process of biofilm matrix assembly and the dynamic interspecies competition between a cariogenic oral pathogen and alkali-producing commensal organism, demonstrating the multiaction potency of this readily available biofilm disruptor.

ACKNOWLEDGMENTS

We thank Dongyeop Kim and Yong Li for helpful discussions and technical assistance.

LaTonya Kilpatrick-Liverman and Peter Santarpia are affiliated with Colgate-Palmolive Co. The funders had no role in the study design, data collection and interpretation, or the decision to submit the work for publication.

We gratefully acknowledge financial support from Colgate-Palmolive Company, Piscataway, NJ. Jinzhi He was supported by a fellowship from the China Scholarship Council. Imaging experiments were performed in the PennVet Imaging Core Facility on instrumentation supported by grant NIH S10RR027128, the School of Veterinary Medicine, the University of Pennsylvania, and the Commonwealth of Pennsylvania.

FUNDING INFORMATION

This work, including the efforts of Hyun Koo, was funded by Colgate-Palmolive Company.

The funders had no role in the study design, data collection and interpretation, or the decision to submit the work for publication.

REFERENCES

1. **Flemming HC, Wingender J.** 2010. The biofilm matrix. Nat Rev Microbiol **8:**623–633.
2. **Koo H, Falsetta ML, Klein MI.** 2013. The exopolysaccharide matrix: a virulence determinant of cariogenic biofilm. J Dent Res **92:**1065–1073. http://dx.doi.org/10.1177/0022034513504218.
3. **Hall-Stoodley L, Costerton JW, Stoodley P.** 2004. Bacterial biofilms: from the natural environment to infectious diseases. Nat Rev Microbiol **2:**95–108. http://dx.doi.org/10.1038/nrmicro821.
4. **Kassebaum NJ, Bernabé E, Dahiya M, Bhandari B, Murray CJL, Marcenes W.** 2015. Global burden of untreated caries: a systematic review and metaregression. J Dent Res **94:**650–658. http://dx.doi.org/10.1177/0022034515573272.
5. **Leme AFP, Koo H, Bellato CM, Bedi G, Cury JA.** 2006. The role of sucrose in cariogenic dental biofilm formation–new insight. J Dent Res **85:**878–887. http://dx.doi.org/10.1177/154405910608501002.
6. **Xiao J, Klein MI, Falsetta ML, Lu B, Delahunty CM, Yates JR, III, Heydorn A, Koo H.** 2012. The exopolysaccharide matrix modulates the interaction between 3D architecture and virulence of a mixed-species oral biofilm. PLoS Pathog **8:**e1002623. http://dx.doi.org/10.1371/journal.ppat.1002623.
7. **Diaz PI, Chalmers NI, Rickard AH, Kong C, Milburn CL, Palmer RJ, Jr, Kolenbrander PE.** 2006. Molecular characterization of subject-specific oral microflora during initial colonization of enamel. Appl Environ Microbiol **72:**2837–2848. http://dx.doi.org/10.1128/AEM.72.4.2837-2848.2006.
8. **Nobbs AH, Lamont RJ, Jenkinson HF.** 2009. *Streptococcus* adherence and colonization. Microbiol Mol Biol Rev **73:**407–450. http://dx.doi.org/10.1128/MMBR.00014-09.
9. **Palmer CA, Kent R, Loo CY, Hughes CV, Stutius E, Pradhan N, Dahlan M, Kanasi E, Arevalo Vasquez SS, Tanner ACR.** 2010. Diet and caries-associated bacteria in severe early childhood caries. J Dent Res **89:**1224–1229. http://dx.doi.org/10.1177/0022034510376543.
10. **Bowen WH, Koo H.** 2011. Biology of *Streptococcus mutans*-derived glucosyltransferases: role in extracellular matrix formation of cariogenic biofilms. Caries Res **45:**69–86. http://dx.doi.org/10.1159/000324598.
11. **Vacca-Smith AM, Bowen WH.** 1998. Binding properties of streptococcal glucosyltransferases for hydroxyapatite, saliva-coated hydroxyapatite, and bacterial surfaces. Arch Oral Biol **43:**103–110. http://dx.doi.org/10.1016/S0003-9969(97)00111-8.
12. **Schilling KM, Bowen WH.** 1992. Glucans synthesized *in situ* in experimental salivary pellicle function as specific binding sites for *Streptococcus mutans*. Infect Immun **60:**284–295.
13. **Banas JA, Vickerman MM.** 2003. Glucan-binding proteins of the oral streptococci. Crit Rev Oral Biol Med **14:**89–99. http://dx.doi.org/10.1177/154411130301400203.
14. **Thurnheer T, Gmür R, Shapiro S, Guggenheim B.** 2003. Mass transport of macromolecules within an *in vitro* model of supragingival plaque. Appl Environ Microbiol **69:**1702–1709. http://dx.doi.org/10.1128/AEM.69.3.1702-1709.2003.

15. **Reese S, Guggenheim B.** 2007. A novel TEM contrasting technique for extracellular polysaccharides in *in vitro* biofilms. Microsc Res Tech **70:** 816–822. http://dx.doi.org/10.1002/jemt.20471.
16. **Lynch DJ, Fountain TL, Mazurkiewicz JE, Banas JA.** 2007. Glucan-binding proteins are essential for shaping *Streptococcus mutans* biofilm architecture. FEMS Microbiol Lett **268:**158–165. http://dx.doi.org/10.1111/j.1574-6968.2006.00576.x.
17. **Featherstone JDB.** 2004. The continuum of dental caries—evidence for a dynamic disease process. J Dent Res **83:**39–42.
18. **Nascimento M, Burne R.** 2014. Caries prevention by arginine metabolism in oral biofilms: translating science into clinical success. Curr Oral Health Rep **1:**79–85. http://dx.doi.org/10.1007/s40496-013-0007-2.
19. **Liu YL, Nascimento M, Burne RA.** 2012. Progress toward understanding the contribution of alkali generation in dental biofilms to inhibition of dental caries. Int J Oral Sci **4:**135–140. http://dx.doi.org/10.1038/ijos.2012.54.
20. **Burne RA, Marquis RE.** 2000. Alkali production by oral bacteria and protection against dental caries. FEMS Microbiol Lett **193:**1–6. http://dx.doi.org/10.1111/j.1574-6968.2000.tb09393.x.
21. **Kleinberg I.** 1970. Regulation of the acid-base metabolism of the dentogingival plaque and its relation to dental caries and periodontal disease. Int Dent J **20:**451–471.
22. **Van Wuyckhuyse BC, Perinpanayagam HER, Bevacqua D, Raubertas RE, Billings RJ, Bowen WH, Tabak LA.** 1995. Association of free arginine and lysine concentrations in human parotid saliva with caries experience. J Dent Res **74:**686–690. http://dx.doi.org/10.1177/00220345950740021001.
23. **Nascimento MM, Gordan VV, Garvan CW, Browngardt CM, Burne RA.** 2009. Correlations of oral bacterial arginine and urea catabolism with caries experience. Oral Microbiol Immun **24:**89–95. http://dx.doi.org/10.1111/j.1399-302X.2008.00477.x.
24. **Nascimento MM, Liu Y, Kalra R, Perry S, Adewumi A, Xu X, Primosch RE, Burne RA.** 2013. Oral arginine metabolism may decrease the risk for dental caries in children. J Dent Res **92:**604–608. http://dx.doi.org/10.1177/0022034513487907.
25. **Sharma S, Lavender S, Woo J, Guo L, Shi W, Kilpatrick L, Gimzewski JK.** 2014. Nanoscale characterization of effect of L-arginine on *S. mutans* biofilm adhesion by atomic force microscopy. Microbiology **160:**1466–1473.
26. **Jakubovics NS, Robinson JC, Samarian DS, Kolderman E, Yassin SA, Bettampadi D, Bashton M, Rickard AH.** 2015. Critical roles of arginine in growth and biofilm development by *Streptococcus gordonii*. Mol Microbiol **97:**281–300. http://dx.doi.org/10.1111/mmi.13023.
27. **Kolderman E, Bettampadi D, Samarian D, Dowd SE, Foxman B, Jakubovics NS, Rickard AH.** 2015. L-Arginine destabilizes oral multispecies biofilm communities developed in human saliva. PLoS One **10:** e0121835. http://dx.doi.org/10.1371/journal.pone.0121835.
28. **Koopman J, Röling WM, Buijs M, Sissons C, ten Cate J, Keijser BF, Crielaard W, Zaura E.** 2014. Stability and resilience of oral microcosms toward acidification and *Candida* outgrowth by arginine supplementation. Microb Ecol **69:**422–433.
29. **Nascimento MM, Browngardt C, Xiaohui X, Klepac-Ceraj V, Paster BJ, Burne RA.** 2014. The effect of arginine on oral biofilm communities. Mol Oral Microbiol **29:**45–54. http://dx.doi.org/10.1111/omi.12044.
30. **Kraivaphan P, Amornchat C, Triratana T, Mateo LR, Ellwood R, Cummins D, DeVizio W, Zhang YP.** 2013. Two-year caries clinical study of the efficacy of novel dentifrices containing 1.5% arginine, an insoluble calcium compound and 1,450 ppm fluoride. Caries Res **47:**582–590. http://dx.doi.org/10.1159/000353183.
31. **Souza MLR, Cury JZ, Tenuta LMA, Zhang YP, Mateo LR, Cummins D, Ellwood RP.** 2013. Comparing the efficacy of a dentifrice containing 1.5% arginine and 1450 ppm fluoride to a dentifrice containing 1450 ppm fluoride alone in the management of primary root caries. J Dent **41:**35–41.
32. **Ajdić D, McShan WM, McLaughlin RE, Savić G, Chang J, Carson MB, Primeaux C, Tian R, Kenton S, Jia H, Lin S, Qian Y, Li S, Zhu H, Najar F, Lai H, White J, Roe BA, Ferretti JJ.** 2002. Genome sequence of *Streptococcus mutans* UA159, a cariogenic dental pathogen. Proc Natl Acad Sci U S A **99:** 14434–14439. http://dx.doi.org/10.1073/pnas.172501299.
33. **Dong Y, Chen YYM, Snyder JA, Burne RA.** 2002. Isolation and molecular analysis of the gene cluster for the arginine deiminase system from *Streptococcus gordonii* DL1. Appl Environ Microbiol **68:**5549–5553. http://dx.doi.org/10.1128/AEM.68.11.5549-5553.2002.
34. **Dige I, Raarup MK, Nyengaard JR, Kilian M, Nyvad B.** 2009. *Actinomyces naeslundii* in initial dental biofilm formation. Microbiology **155:** 2116–2126. http://dx.doi.org/10.1099/mic.0.027706-0.
35. **Sztajer H, Szafranski SP, Tomasch J, Reck M, Nimtz M, Rohde M, Wagner-Dobler I.** 2014. Cross-feeding and interkingdom communication in dual-species biofilms of *Streptococcus mutans* and *Candida albicans*. ISME J **8:**2256–2271. http://dx.doi.org/10.1038/ismej.2014.73.
36. **Ren Z, Cui T, Zeng J, Chen L, Zhang W, Xu X, Cheng L, Li M, Li J, Zhou X, Li Y.** 2016. Molecule targeting glucosyltransferase inhibits *Streptococcus mutans* biofilm formation and virulence. Antimicrob Agents Chemother **60:**126–135. http://dx.doi.org/10.1128/AAC.00919-15.
37. **Bamford CV, d'Mello A, Nobbs AH, Dutton LC, Vickerman MM, Jenkinson HF.** 2009. *Streptococcus gordonii* modulates *Candida albicans* biofilm formation through intergeneric communication. Infect Immun **77:**3696–3704. http://dx.doi.org/10.1128/IAI.00438-09.
38. **Aspiras MB, Kazmerzak KM, Kolenbrander PE, McNab R, Hardegen N, Jenkinson HF.** 2000. Expression of green fluorescent protein in *Streptococcus gordonii* DL1 and its use as a species-specific marker in coadhesion with *Streptococcus oralis* 34 in saliva-conditioned biofilms *in vitro*. Appl Environ Microbiol **66:**4074–4083. http://dx.doi.org/10.1128/AEM.66.9.4074-4083.2000.
39. **Tanzer JM, Thompson A, Sharma K, Vickerman MM, Haase EM, Scannapieco FA.** 2012. *Streptococcus mutans* out-competes *Streptococcus gordonii in vivo*. J Dent Res **91:**513–519. http://dx.doi.org/10.1177/0022034512442894.
40. **Koo H, Xiao J, Klein MI, Jeon JG.** 2010. Exopolysaccharides produced by *Streptococcus mutans* glucosyltransferases modulate the establishment of microcolonies within multispecies biofilms. J Bacteriol **192:**3024–3032. http://dx.doi.org/10.1128/JB.01649-09.
41. **Jeon JG, Pandit S, Xiao J, Gregoire S, Falsetta ML, Klein MI, Koo H.** 2011. Influences of *trans-trans* farnesol, a membrane targeting sesquiterpenoid, on *Streptococcus mutans* physiology and survival within mixed-species oral biofilms. Int J Oral Sci **3:**98–106. http://dx.doi.org/10.4248/IJOS11038.
42. **Cury JA, Koo H.** 2007. Extraction and purification of total RNA from *Streptococcus mutans* biofilms. Anal Biochem **365:**208–214. http://dx.doi.org/10.1016/j.ab.2007.03.021.
43. **Koo H, Hayacibara MF, Schobel BD, Cury JA, Rosalen PL, Park YK, Vacca-Smith AM, Bowen WH.** 2003. Inhibition of *Streptococcus mutans* biofilm accumulation and polysaccharide production by apigenin and *tt*-farnesol. J Antimicrob Chemother **52:**782–789. http://dx.doi.org/10.1093/jac/dkg449.
44. **Klein MI, DeBaz L, Agidi S, Lee H, Xie G, Lin AHM, Hamaker BR, Lemos JA, Koo H.** 2010. Dynamics of *Streptococcus mutans* transcriptome in response to starch and sucrose during biofilm development. PLoS One **5:**e13478.
45. **Gao L, Zhuang J, Nie L, Zhang J, Zhang Y, Gu N, Wang T, Feng J, Yang D, Perrett S, Yan X.** 2007. Intrinsic peroxidase-like activity of ferromagnetic nanoparticles. Nat Nanotechnol **2:**577–583. http://dx.doi.org/10.1038/nnano.2007.260.
46. **Hale JDF, Ting YT, Jack RW, Tagg JR, Heng NCK.** 2005. Bacteriocin (mutacin) production by *Streptococcus mutans* genome sequence reference strain UA159: elucidation of the antimicrobial repertoire by genetic dissection. Appl Environ Microbiol **71:**7613–7617. http://dx.doi.org/10.1128/AEM.71.11.7613-7617.2005.
47. **Kreth J, Zhang Y, Herzberg MC.** 2008. Streptococcal antagonism in oral biofilms: *Streptococcus sanguinis* and *Streptococcus gordonii* interference with *Streptococcus mutans*. J Bacteriol **190:**4632–4640. http://dx.doi.org/10.1128/JB.00276-08.
48. **Merritt J, Qi F.** 2012. The mutacins of *Streptococcus mutans* regulation and ecology. Mol Oral Microbiol **27:**57–69. http://dx.doi.org/10.1111/j.2041-1014.2011.00634.x.
49. **Barnard JP, Stinson MW.** 1999. Influence of environmental conditions on hydrogen peroxide formation by *Streptococcus gordonii*. Infect Immun **67:**6558–6564.
50. **Takahashi N, Nyvad B.** 2011. The role of bacteria in the caries process: ecological perspectives. J Dent Res **90:**294–303. http://dx.doi.org/10.1177/0022034510379602.
51. **Bowen W.** 2013. The Stephan curve revisited. Odontology **101:**2–8. http://dx.doi.org/10.1007/s10266-012-0092-z.
52. **Zheng X, Cheng X, Wang L, Qiu W, Wang S, Zhou Y, Li M, Li Y, Cheng L, Li J, Zhou X, Xu X.** 2014. Combinatorial effects of arginine and fluoride on oral bacteria. J Dent Res **94:**344–353.

53. **Marsh PD, Head DA, Devine DA.** 2015. Ecological approaches to oral biofilms: control without killing. Caries Res **49**(Suppl 1)**:**46–54.
54. **Hwang G, Klein MI, Koo H.** 2014. Analysis of the mechanical stability and surface detachment of mature *Streptococcus mutans* biofilms by applying a range of external shear forces. Biofouling **30:**1079–1091. http://dx.doi.org/10.1080/08927014.2014.969249.
55. **Hope CK, Wilson M.** 2004. Analysis of the effects of chlorhexidine on oral biofilm vitality and structure based on viability profiling and an indicator of membrane integrity. Antimicrob Agents Chemother **48:**1461–1468. http://dx.doi.org/10.1128/AAC.48.5.1461-1468.2004.
56. **Jakubovics NS, Gill SR, Iobst SE, Vickerman MM, Kolenbrander PE.** 2008. Regulation of gene expression in a mixed-genus community: stabilized arginine biosynthesis in *Streptococcus gordonii* by coaggregation with *Actinomyces naeslundii*. J Bacteriol **190:**3646–3657. http://dx.doi.org/10.1128/JB.00088-08.
57. **Guo L, Hu W, He X, Lux R, McLean J, Shi W.** 2013. Investigating acid production by *Streptococcus mutans* with a surface-displayed pH-sensitive green fluorescent protein. PLoS One **8:**e57182. http://dx.doi.org/10.1371/journal.pone.0057182.
58. **Zero DT, Fu J, Anne KM, Cassata S, McCormack SM, Gwinner LM.** 1992. An improved intra-oral enamel demineralization test model for the study of dental caries. J Dent Res **71:**871–878.